

# A model for coupling within-host and between-host dynamics in an infectious disease

Zhilan Feng · Jorge Velasco-Hernandez ·  
Brenda Tapia-Santos · Maria Conceição A. Leite

Received: 27 May 2011 / Accepted: 26 November 2011 / Published online: 21 December 2011  
© Springer Science+Business Media B.V. 2011

**Abstract** Studies on the modeling of the coupled dynamics of infectious diseases at both the population level (the epidemic process or between-host dynamics) and at the cell level (the early viremia or within-host dynamics) are scarce. Most of them deal with these two processes separately by postulating assumptions that render them decoupled.

In this work, we present a new model that allows the two dynamic processes to explicitly depend on each other. It is shown that new properties can emerge from the coupled system and more complex dynamics may be expected.

**Keywords** Disease persistence · Early viremia · Multistability · Multiparameter bifurcation

## 1 Introduction

For infectious diseases, such as HIV infection, two key processes play important roles in the study of the host-parasite interaction. One is the epidemic process that involves disease transmission between hosts, and the other is the immunological process related to the virus-cell interaction at the level of an individual host. Although an increasing number of mathematical models have been developed to study the transmission dynamics of these diseases, most of them treat these two processes separately. Viral dynamic models (e.g., Anderson and May [1], De Boer and Perelson [4], Nowak and May [9, 10], Perelson et al. [11], Perelson and Nelson [12], Regoes et al. [14], Wodarz [16]) consider the within-host dynamics independent of the interaction at the population level), whereas epidemic models of population dynamics (e.g., Anderson and May [1], Thieme [15], and references therein) consider the interaction between susceptible and infected hosts without an explicit link to the viral dynamics within hosts (by implicitly assuming that all infectious hosts have the same constant viral load, and hence the same infectivity). When the two processes are decoupled, the mathematical models are in general easier to analyze. However, there remain questions that can only be addressed by using models which explicitly

---

Z. Feng  
Department of Mathematics, Purdue University, West  
Lafayette, USA  
e-mail: [zfeng@math.purdue.edu](mailto:zfeng@math.purdue.edu)

J. Velasco-Hernandez (✉)  
Programa de Matemáticas Aplicadas y Computación,  
Instituto Mexicano del Petróleo, México City, México  
e-mail: [jx.velasco@gmail.com](mailto:jx.velasco@gmail.com)

B. Tapia-Santos  
Facultad de Matemáticas, Universidad Veracruzana,  
México City, México  
e-mail: [bretasa@gmail.com](mailto:bretasa@gmail.com)

M.C.A. Leite  
Department of Mathematics, University of Oklahoma,  
Norman, USA  
e-mail: [mleite@ou.edu](mailto:mleite@ou.edu)

**Table 1** Biological quantities and parameter values used in simulations

Parameter	Value	Description	Reference
$\Lambda_c$	$10^4 \frac{\text{cells}}{\text{time}}$	Recruitment rate of uninfected cells	[2]
$\mu_c$	$0.01 \frac{1}{\text{time}}$	Death rate of uninfected cells	[2]
$\delta_c$	$1 \frac{1}{\text{time}}$	Death rate of infected cells	[8]
$p$	$5000 \frac{\text{viruses}}{\text{time}\cdot\text{cell}}$	Viral production rate	[5]
$c$	$23 \frac{1}{\text{time}}$	Clearance rate of free virus	[13]
$\mu$	$\frac{1}{70 \times 365} \frac{1}{\text{time}}$	Host natural death rate	
$\Lambda$	$5000\mu \frac{\text{hosts}}{\text{time}}$	Host recruitment rate	
$\mathcal{R}_v$		Within-host reproduction number	
$\mathcal{R}_h$		Between-host reproduction number	
$\mathcal{R}_h^\beta$		“Isolated” host reproduction number	
$\mathcal{R}_{v0} = \mathcal{R}_v \hat{N}$		“Isolated” virus reproduction number	
$\mathcal{R}_{ve}^\pm = \frac{\hat{I}_\pm \mathcal{R}_{v0}}{\hat{N}}$		“Effective” reproduction number	
$\mathcal{R}_{h \max}$		Maximum of $\mathcal{R}_h$ for stability	

link the two processes. Such questions include: (i) To what extent does the within-host dynamics influence the disease dynamics at the population level? (ii) What is the effect of population dynamics of disease transmission on the viral dynamics at the individual level? (iii) Will the model predictions regarding the evolution of virulence and the basic reproduction number of the pathogen be altered if the two processes are *dynamically* linked? Some recent studies have incorporated the parasite characteristics within individual hosts into the between-host dynamics. For example, Gilchrist and Coombs [7] use a nested model to evaluate the direction of natural selection (in the study of evolution of virulence) at the within- and between-host levels. In this nested model, the within-host system is assumed to be independent of the transmission dynamics at the population level.

In this paper, we propose a model with an explicit linkage between the epidemiological and immunological dynamics. This model builds upon the approach of Gilchrist and Coombs [7] by relaxing the steady-state assumption for the immune system. A model considered in [3] also relaxed the steady-state assumption by incorporating the immunological dynamics and linking the prevalence level of disease to the average viral load at the within-host level. Their results arise mainly from numerical computations. To the best of our knowledge, all existing models that are intended to couple immunological and epidemiological dynamics

confront the difficulty as to what are the more appropriate ways to incorporate epidemiological dynamics into the within-host cellular process. It is clear that the prevalence of a disease should play a role in influencing the pathogen behavior within individual hosts, although the specific mechanism is elusive (see Fraser et al. [6]).

Our model incorporates not only the dependence of epidemics on the viral dynamics, but also the dependence of the within-host dynamics on the between-host dynamics;. Particularly, it allows the within-host viral load to vary as the epidemic level changes. Our approach makes it possible to perform a bifurcation analysis of both the infection-free and the interior equilibria. We also illustrate our findings using numerical simulations. The model consists of ordinary differential equations that represent average or mean field approximations of the true time and spatial scales of the object of study. An alternative formulation could involve an infection-age structured model. However, any attempt in this direction would not only be mathematically challenging but also require a multitude of parameters and, necessarily, data to validate it. Given the nature of the phenomena at hand, these requirements may be very difficult to satisfy. Therefore, the approach of using simpler models may have advantages over uses of agent based or computational models that can be very complex while providing very limited theoretical insights.

## 2 Model assumptions and construction

Our model is an extension of the “nested model” considered in Gilchrist and Coombs [7]. We first provide some background information and the motivation of our model by discussing a few unique features associated with the nested model.

### 2.1 Some background information about the nested model

The nested model consists of two submodels, one for the epidemiology at population level, and the other for the viral dynamics within an individual host. The between-host system is a standard  $SI$  type model, where  $S$  and  $I$  denote the numbers of susceptible and infected (infectious) hosts, respectively. The  $SI$  system reads

$$\begin{aligned} \dot{S} &= b(S, I) - \beta(V)SI - \mu S, \\ \dot{I} &= \beta(V)SI - \mu I, \end{aligned} \tag{1}$$

where  $b(S, I)$  is the recruitment rate of uninfected hosts (possibly density dependent),  $\mu$  is the per capita natural death rate,  $\beta(V)$  is the transmission rate and is assumed to be an increasing function of  $V$  with  $\beta(0) = 0$ , and  $V$  denotes the viral load in a single infected host. We point out that (1) assumes an identical transmission rate for all infected hosts, which implies that the viral load within hosts are the same.

The within-host system in the nested model reads

$$\begin{aligned} \dot{T} &= \Lambda_c - kTV - \mu_c T, \\ \dot{T}^* &= kTV - (\mu_c + \delta_c)T^*, \\ \dot{V} &= pT^* - cV, \end{aligned} \tag{2}$$

where  $T$  is the density of uninfected host cells (e.g.,  $T$  cells in the case of HIV) susceptible to infection,  $T^*$  is the density of productively infected host cells, and  $V$  is the density of free (infectious) virions within a host.  $\Lambda_c$  is the rate at which new target cells are created,  $k$  is the infection rate of  $T$  cells by an infectious virus,  $\mu_c$  is the per capita background mortality of cells,  $\delta_c$  is the extra per capita cell mortality induced by viruses (virulence), and  $p$  and  $c$  are the virion production and clearance rates, respectively. All parameters are assumed to be constant (i.e., density independent). Note that the mass action law is used in both subsystems. Observe that although the system at the epidemiological level (1) is dependent on the variable  $V$  from the within-host system, the cell-virus system (2) does not depend

on the epidemiological level represented by  $I$ . This lack of dependence of (2) on (1) may lead to inconsistent outcomes. One example is described below.

If  $b(S, I) = \Lambda$ , then the total host population  $N(t) = S(t) + I(t) \rightarrow \Lambda/\mu$  as  $t \rightarrow \infty$ . The asymptotic constant  $\Lambda/\mu$  will be denoted by  $\hat{N}$  in the remainder of this paper. System (1) always has the infection-free equilibrium  $E_0 = (\hat{N}, 0)$ . Let  $\tilde{E} = (\tilde{S}, \tilde{I})$  (with  $\tilde{I} > 0$ ) denote an endemic equilibrium. When  $\tilde{E}$  exists, the population level of infection is

$$\tilde{I} = \frac{\Lambda}{\mu} \left( 1 - \frac{1}{\mathcal{R}_h^{\beta(V)}} \right), \tag{3}$$

where

$$\mathcal{R}_h^{\beta(V)} = \frac{\beta(V)\hat{N}}{\mu} \tag{4}$$

is the basic reproductive number associated with the between-host system (1) for a given viral load  $V$ . It is easy to see from (3) that  $\tilde{E}$  exists only if  $\mathcal{R}_h^{\beta(V)} > 1$  and  $V > 0$ . When  $\mathcal{R}_h^{\beta(V)} < 1$ ,  $E_0$  is a global attractor, i.e.,

$$I(t) \rightarrow 0 \quad \text{as } t \rightarrow \infty \quad \text{if } \mathcal{R}_h^{\beta(V)} < 1. \tag{5}$$

For the within-host system, whether the virus population will go extinct or persist is determined by a separate set of parameters. If the nontrivial equilibrium  $\tilde{U} = (\tilde{T}, \tilde{T}^*, \tilde{V})$  (with  $\tilde{T}^* > 0$ ) exists, then the viral load is

$$\tilde{V} = \frac{\mu_c}{k} (\mathcal{R}_v - 1), \tag{6}$$

where

$$\mathcal{R}_v = \frac{\Lambda_c k p}{c \mu_c (\mu_c + d_c)}$$

is the basic reproductive number for the within-host system. It can be shown that  $\tilde{U}$  exists and is globally stable if and only if  $\mathcal{R}_v > 1$ . Therefore,

$$V(t) \rightarrow \tilde{V} \quad \text{as } t \rightarrow \infty \quad \text{if } \mathcal{R}_v > 1.$$

Notice that  $\mathcal{R}_v$  does not depend on either the parameters or variables associated with the between-host system (1). It follows that, regardless of any dynamic changes at the host level, if  $\mathcal{R}_v > 1$ , then the viral load within a host will stabilize at the level  $\tilde{V} > 0$  given in (6).

Now we consider (1) for a particular case, in which  $\beta(V)$  is a linear function of  $V$ , i.e.,

$$\beta(V) = \beta_0 V, \tag{7}$$

where  $\beta_0$  is a constant. Using (7) and substituting  $\tilde{V} > 0$  (see (6)) into the formula for  $\mathcal{R}_h^{\beta(V)}$  as given in (4), we can determine parameter values of  $\beta_0, \delta$  and  $\hat{N}$  for which  $\mathcal{R}_h^{\beta(V)} < 1$ . In this case,  $I(t) \rightarrow 0$  as  $t \rightarrow \infty$ .

The above observation suggests that if  $\mathcal{R}_h^{\beta(V)} < 1$  and  $\mathcal{R}_v > 1$ , then the nested model predicts that the between-host dynamics will stabilize at the infection-free steady state (i.e.,  $\tilde{I} = 0$ ), while the within-host dynamics will stabilize at a steady state with a positive viral level  $\tilde{V}$  which does not depend on any factors at the population level.

Some may argue that the above mentioned outcome is not inconsistent since even though the number of infected hosts is changing, the equilibrium viral load in a single infected host can still remain at the same level since viral dynamics should not depend on how many hosts are infected. This argument may be valid if one is focusing only on the within-host dynamics of a single host on a time scale that is much shorter than the epidemiological process. However, if the purpose of coupling the two processes is to study long-term (e.g., on the evolutionary, or even ecological time scale) dynamics, then multiple generations of host transmission need to be considered. Therefore, it is more reasonable to allow the viral dynamics within host to change over time, as in the work by Coombs, Gilchrist, and Ball [3], and to be influenced by the selection pressure from the epidemiological process.

### 2.2 Coupling the systems

To link the two processes, we need to explore further the connection between them, especially the effect of between-host on the within-host dynamics.

We will adopt the *SI* system (1) for the epidemiological process, and focus on how the cell-virus system should depend on  $I$ , the prevalence level in the host population. Our approach is to start with  $n$  systems, each of which governs the viral dynamics of a single host. These systems will then be used to derive an ‘average’ system that will describe the average viral load and cell densities.

In what follows, we round up  $\hat{N} = \Lambda/\mu$  to its nearest integer value, and look at the full system at this demographic equilibrium. For each host  $j$  ( $j = 1, 2, \dots, \hat{N}$ ), let  $V_j$  denote the viral load of infected host, and let  $T_j$  and  $T_j^*$  denote the amount of healthy and infected T cells, respectively. Let  $V_{av}, T_{av}^*$ , and  $T_{av}$  denote the average viral load, average amount of

infected T cells, and average amount of uninfected T cells, respectively, defined as

$$\begin{aligned} V_{av} &= \frac{1}{\hat{N}} \sum_{j=1}^{\hat{N}} V_j, & T_{av}^* &= \frac{1}{\hat{N}} \sum_{j=1}^{\hat{N}} T_j^*, \\ T_{av} &= \frac{1}{\hat{N}} \sum_{j=1}^{\hat{N}} T_j. \end{aligned} \tag{8}$$

Consider the case when  $0 < I < \hat{N}$  (i.e., there is a positive number of infected hosts but not all hosts are infected). Without loss of generality, assume that only individuals with indices  $j = 1, 2, \dots, I$  are infected. That is,  $V_j > 0$  for  $j = 1, 2, \dots, I$  and  $V_j = 0$  for  $j = I + 1, \dots, \hat{N}$ . For each individual, the within-host dynamics is described by the following system

$$\begin{aligned} \dot{T}_j &= \Lambda_c - \hat{k}T_jV_j - \mu_cT_j, \\ \dot{T}_j^* &= \hat{k}T_jV_j - (\mu_c + \delta_c)T_j^*, \\ \dot{V}_j &= pT_j^* - cV_j, \quad j = 1, 2, \dots, \hat{N}. \end{aligned} \tag{9}$$

$\Lambda_c$  is the recruitment rate of healthy T cells,  $\hat{k}$  is the rate at which a T cell becomes infected when contacting an infectious virus,  $\mu_c$  is the per capita background mortality of cells,  $\delta_c$  is the viral induced per capita cell death rate (virulence), and  $p$  and  $c$  are the viral shedding and clearance rates, respectively. All parameters are assumed to be the same among the hosts. Note that, implicitly, the immunological system (8)–(9) depends on  $I$ , the number of infected persons.

To derive an equation for the average  $T_{av}$ , we sum over the whole population and use (8) and the  $T_j$  equation in (9) to get

$$\begin{aligned} \dot{T}_{av} &= \frac{1}{\hat{N}} \sum_{j=1}^{\hat{N}} \dot{T}_j \\ &= \Lambda_c - \hat{k} \frac{1}{\hat{N}} \sum_{j=1}^{\hat{N}} T_j V_j - \mu_c T_{av} \\ &= \Lambda_c - \hat{k} \frac{1}{\hat{N}} \sum_{j=1}^I T_j V_j - \mu_c T_{av}, \end{aligned} \tag{10}$$

where the term

$$\sum_{j=1}^I T_j V_j$$

represents the total incidence.

Since we want to preserve the mass-action law for the averages, we make the following assumption on the relation between the total contact rate and the average contact rate:

$$\sum_{j=1}^I V_j T_j = \Theta(I) T_{av} V_{av}.$$

The function  $\Theta$  depends on the detailed knowledge of the way in which population level processes affect the within-host dynamics. Since this knowledge is still very scarce (for example Fraser et al. [6] where there is evidence of this connection) we propose here the simplest linear relation that preserves the mass action law for the contact rates incorporated in (9):

$$\Theta(I) = \theta I$$

where  $\theta$  is a scaling constant. In this case, the term  $\sum_{j=1}^I V_j T_j$  in (10) can be replaced by  $\theta I T_{av} V_{av}$ , i.e.,

$$\sum_{j=1}^I V_j T_j = \theta I T_{av} V_{av}.$$

Expanding the RHS of the above expression, we obtain that

$$\begin{aligned} \theta I T_{av} V_{av} &= \frac{\theta I}{\hat{N}^2} \left( \sum_{i=1}^{\hat{N}} V_i T_i + \sum_{i \neq j} V_i T_j \right) \\ &= \frac{\theta I}{\hat{N}^2} \left( f(V_i, T_i) + \sum_{i \neq j} V_i T_j \right) \end{aligned}$$

where we have defined

$$f(V_i, T_i) = \sum_{i=1}^I V_i T_i.$$

Let  $\hat{k} = \theta$ . Then

$$\frac{\hat{k}}{\hat{N}} \sum_{j=1}^I V_j T_j = \frac{\theta}{\hat{N}} f(V_i, T_i) \geq \frac{\theta}{\hat{N}} \frac{I}{\hat{N}} f(V_i, T_i),$$

and, therefore, we are assuming that the quantity  $\frac{\theta I}{\hat{N}^2} \sum_{i \neq j} V_i T_j$  is small enough as to make the substitution with verges a reasonable approximation.

Thus, from (10), we obtain the following equation for  $T_{av}$ :

$$\dot{T}_{av} = \Lambda_c - k I T_{av} V_{av} - \mu_c T_{av},$$

where

$$k = \frac{\hat{k} \theta}{\hat{N}}.$$

Similarly, from the  $T_j^*$  and  $V_j$  equations in (9) we get

$$\begin{aligned} \dot{T}_{av}^* &= k I T_{av} V_{av} - (\mu_c + \delta_c) T_{av}^*, \\ \dot{V}_{av} &= p T_{av}^* - c V_{av}. \end{aligned}$$

The above gives the following system for the averages:

$$\begin{aligned} \dot{T}_{av} &= \Lambda_c - k I T_{av} V_{av} - \mu_c T_{av} \\ \dot{T}_{av}^* &= k I T_{av} V_{av} - (\mu_c + \delta_c) T_{av}^*, \\ \dot{V}_{av} &= p T_{av}^* - c V_{av}. \end{aligned} \tag{11}$$

### 3 Model analysis and emerging properties

First we consider the case in which the host recruitment rate is a constant  $b(S, I) = \Lambda$ , and the host infection rate is linear, i.e.,  $\beta(V) = \beta_0 V$  where  $\beta_0$  is a constant. In addition, the analysis below is performed for the case when  $\theta = 1$ . In this case, if we drop the subscript  $av$  for average (i.e.,  $T = T_{av}$ ,  $T_{av}^* = T^*$ ,  $V = V_{av}$ ) and the subscript in  $\beta_0$  then the coupled system is

$$\begin{aligned} \dot{S} &= \Lambda - \beta V S I - \mu S, \\ \dot{I} &= \beta V S I - \mu I, \\ \dot{T} &= \Lambda_c - k I T V - \mu_c T, \\ \dot{T}^* &= k I T V - (\mu_c + \delta_c) T^*, \\ \dot{V} &= p T^* - c V. \end{aligned} \tag{12}$$

System (12) has at most three biologically feasible equilibria. The infection-free equilibrium  $E_0 = (\hat{N}, 0, T_0, 0, 0)$  always exists, where  $\hat{N} = \Lambda/\mu$  and  $T_0 = \Lambda_c/\mu_c$  are the total host and target cell population sizes, respectively, in the absence of infection. Let  $\hat{E} = (\hat{S}, \hat{I}, \hat{T}, \hat{T}^*, \hat{V})$  denote an interior equilibrium (i.e., all components are positive) of the coupled system. The existence of  $\hat{E}$  is determined by relations involving the following between- and within-host reproduction numbers

$$\mathcal{R}_h = \mathcal{R}_h^\beta \varphi = \frac{\beta \varphi \hat{N}}{\mu}, \quad \mathcal{R}_v = \frac{k p T_0}{(\mu_c + \delta_c) c} \tag{13}$$

with

$$\varphi = \frac{\mu_c}{k} \quad \text{and} \quad \mathcal{R}_h^\beta = \frac{\beta \hat{N}}{\mu}.$$

The quantity  $1/\varphi = k/\mu_c$  gives the number of effective contacts per viral load per person during the lifetime of a cell and has units of people times viral load. The factor  $\varphi$  in  $\mathcal{R}_h$  represents the effect of the viral

load on the force of infection at the host level.  $\mathcal{R}_v$  is the basic reproductive number of the virus for the within-host subsystem.

An important new feature of the coupled system (12) is that it has multiple endemic equilibria and, therefore, it can generate more diverse dynamics than the two subsystems in isolation. The host subsystem can be decoupled from (12) by taking  $V$  constant. On the other hand, the independent cell-virus system can be obtained by taking  $I$  constant. For the between-host subsystem, the basic reproductive number is  $\mathcal{R}_h^\beta$  defined in (13). This subsystem has a unique stable interior equilibrium if  $\mathcal{R}_h^\beta > 1$  and no interior equilibrium if  $\mathcal{R}_h^\beta < 1$ .

For the cell-virus subsystem, noticing that  $k = \hat{k}\theta/\hat{N}$  and  $\hat{N} = \Lambda/\mu$  at the disease-free equilibrium, the basic reproductive number is

$$\mathcal{R}_{v0} = \frac{\hat{k}\theta p T_0}{(\mu_c + \delta_c)c} = \mathcal{R}_v \hat{N}.$$

There is a unique stable interior equilibrium if  $\mathcal{R}_{v0} > 1$  and no interior equilibrium if  $\mathcal{R}_{v0} < 1$ .

We show below that some of the threshold conditions (in terms of the reproductive numbers and the number of interior equilibria) for (12) differ from those obtained by decoupling the between- and within-host systems.

### 3.1 Multiple endemic equilibria and bistability

In this section, we state the main results from the mathematical model. This section is somewhat technical, but we provide the mathematical proofs in the supplementary section. Denote an interior equilibrium by  $\hat{E}_\pm = (\hat{S}_\pm, \hat{I}_\pm, \hat{T}_\pm, \hat{T}_\pm^*, \hat{V}_\pm)$  with  $\hat{I}_\pm > 0$ . Setting the right-hand side of equations in (12) equal to zero yields two nontrivial solutions for the components of  $\hat{E}_\pm$ :

$$\begin{aligned} \hat{S}_\pm &= \hat{N}(1 - \hat{y}_\pm), & \hat{I}_\pm &= \hat{y}_\pm \hat{N}, \\ \hat{T}_\pm &= \frac{T_0}{\hat{y}_\pm \mathcal{R}_{v0}}, & \hat{T}_\pm^* &= \frac{c\hat{V}_\pm}{p}, \\ \hat{V}_\pm &= \frac{\mu_c}{k\hat{N}\hat{y}_\pm}(\hat{y}_\pm \mathcal{R}_{v0} - 1), \end{aligned} \tag{14}$$

where  $\mathcal{R}_{v0} = \mathcal{R}_v \hat{N}$  and  $\hat{y}_\pm$  are the solutions of the quadratic equation

$$\mathcal{R}_{v0}y^2 + By + 1 = 0 \tag{15}$$

with

$$B = \frac{\hat{N}}{\mathcal{R}_h} - \mathcal{R}_{v0} - 1. \tag{16}$$

Explicit formulas for  $\hat{y}_\pm$  are given by

$$\hat{y}_\pm = \frac{1}{2\mathcal{R}_{v0}} \left( -B \pm \sqrt{B^2 - 4\mathcal{R}_{v0}} \right). \tag{17}$$

For  $\hat{E}_\pm$  to be biologically feasible, we need to show that  $\hat{y}_\pm$  are real numbers and

$$\begin{aligned} \hat{S}_\pm &> 0, & 0 < \hat{I}_\pm < \hat{N}, & \hat{V}_\pm > 0, \\ \hat{S}_\pm + \hat{I}_\pm &= \hat{N}. \end{aligned} \tag{18}$$

Before we proceed to the statement of our results, we first define two quantities that play a definitive role in the existence or lack of existence of interior equilibria. Let

$$\mathcal{R}_{ve}^\pm = \frac{\hat{I}_\pm}{\hat{N}} \mathcal{R}_{v0} = \frac{1}{2} \left( -B \pm \sqrt{B^2 - 4\mathcal{R}_{v0}} \right), \tag{19}$$

where  $B$  is given in (16). The quantities  $\mathcal{R}_{ve}^\pm$  simplify the mathematical expressions in the corollaries below.

Corollary 1 below establishes that the existence of interior equilibrium points depends on two threshold conditions:

$$\mathcal{R}_{ve}^- = \frac{\hat{I}_-}{\hat{N}} \mathcal{R}_{v0} > 1 \quad \text{and} \quad \mathcal{R}_h \geq F(\mathcal{R}_{v0}), \tag{20}$$

where  $\mathcal{R}_{ve}^-$  is as in (19) and we define

$$F(\mathcal{R}_{v0}) = \frac{\hat{N}}{(\sqrt{\mathcal{R}_{v0}} - 1)^2}. \tag{21}$$

Note that the function  $F(\mathcal{R}_{v0})$  above is unbounded with the property that

$$F(\mathcal{R}_{v0}) \rightarrow \infty \quad \text{as} \quad \mathcal{R}_{v0} \rightarrow 1,$$

pushing  $R_h$  to infinity. Since  $R_h$  has to be a positive real number we introduce an upper bound for it, the maximum value of  $\mathcal{R}_h$  denoted by  $\mathcal{R}_{h \max}$ .

Note that the first inequality in (20) implies that  $\mathcal{R}_{ve}^+ > 1$  (always), and that  $\mathcal{R}_{v0} > \mathcal{R}_{ve\pm} > 1$  if  $\hat{E}_\pm$  exist.

The condition  $\mathcal{R}_{ve}^- = \frac{\hat{I}_-}{\hat{N}} \mathcal{R}_{v0} > 1$  indicates that the within-host dynamics is determined by the within-host viral reproductive number  $\mathcal{R}_{v0}$  scaled by the fraction of infected host in the population ( $\hat{I}_\pm/\hat{N}$ ). The existence of interior equilibria for  $\mathcal{R}_{ve}^- > 1$  derives from the assumption that  $kIV = \hat{k}\theta IV/\hat{N}$ .

Corollary 1 also states that if  $\hat{E}_\pm$  exist, then the total number of infected hosts at equilibrium is limited to



the interval  $\frac{\hat{N}}{\mathcal{R}_{v0}} < \hat{I}_{\pm} < \hat{N}$ . However, when the value of  $\mathcal{R}_{v0}$  increases the set of feasible  $\hat{I}_{\pm}$  also increases, implying that high values of  $\mathcal{R}_{v0}$  improve the virus population survival.

Corollary 2 displays the nature of the stability of all equilibrium points. When interior equilibria exist one of them is locally asymptotically stable and the other unstable. In this case, the DFE is locally asymptotically stable, thus making the global dynamics of the system dependent on the initial conditions. When the interior equilibria do not exist, the only equilibrium is the disease-free state.

**Corollary 1** Let  $F(\mathcal{R}_{v0})$  be the function given in (21).

- (i) If  $\mathcal{R}_{ve}^- > 1$ , then system (12) has
  - (a) no interior equilibrium if  $\mathcal{R}_h < F(\mathcal{R}_{v0})$ ;
  - (b) a unique interior equilibrium if  $\mathcal{R}_h = F(\mathcal{R}_{v0})$ ;
  - (c) two interior equilibria if  $F(\mathcal{R}_{v0}) < \mathcal{R}_h \leq \mathcal{R}_{hmax}$ .
- (ii) If  $\mathcal{R}_{ve}^+ \leq 1$ , then system (12) has no interior equilibrium.
- (iii) Moreover, if  $\hat{E}_{\pm}$  exist and  $\mathcal{R}_{ve}^- > 1$  then

$$\frac{\hat{N}}{\mathcal{R}_{v0}} < \hat{I}_{\pm} < \hat{N} \tag{22}$$

where  $\hat{I}_{\pm} = \hat{y}_{\pm} \hat{N}$  and  $\hat{y}_{\pm}$  are the positive solutions of the quadratic equation given in (17).

A proof of Corollary 1 can be found in the supplementary material.

Note that the condition  $\mathcal{R}_{v0} > 1$ , required for the persistence of the virus population when studying only the dynamics of cell-virus system, is no longer sufficient in the coupled system. This is a consequence of linking the between- and within-host systems. In the coupled system, when the isolated within-host reproductive number  $\mathcal{R}_{v0}$  is greater than one, it is still possible for the infection to go extinct in the whole system. This can occur in the following two scenarios: (1) if  $\mathcal{R}_{v0} > 1$ , but  $\mathcal{R}_{ve}^- < 1$ ; (2) if the between-host reproductive number is not high enough (e.g.,  $\mathcal{R}_h \leq F(\mathcal{R}_{v0})$ ).

Figure 1 shows how the infection level of hosts depends on  $\mathcal{R}_h$  and  $\mathcal{R}_{v0}$ . It illustrates that  $\hat{E}_{\pm}$  exist only for  $\mathcal{R}_h \geq F(\mathcal{R}_{v0})$ , and that the critical value of  $\mathcal{R}_h$  for the existence of  $\hat{E}_{\pm}$  is reduced as  $\mathcal{R}_{v0}$  increases (see Table 1 for parameter values).

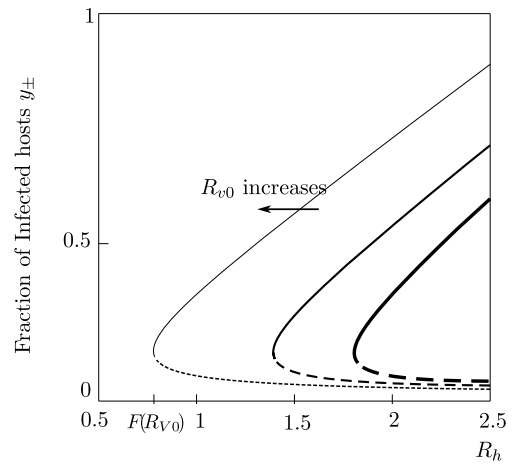


**Fig. 1** Bifurcation diagram for the interior equilibria  $\hat{E}_{\pm}$  versus the parameter  $\mathcal{R}_h$  for various values of  $\mathcal{R}_{v0}$ . The solid curves denote  $\hat{I}_+/\hat{N}$  and the dashed curves denote  $\hat{I}_-/\hat{N}$  for different values of  $\mathcal{R}_{v0}$ . The tick label  $F(\mathcal{R}_{v0})$  on the  $\mathcal{R}_h$  axis represents the critical value  $\mathcal{R}_h = F(\mathcal{R}_{v0})$  for the curve corresponding to the largest  $\mathcal{R}_{v0}$ . To the left of this point, there are no interior equilibria.  $\hat{E}_{\pm}$  exists only for  $\mathcal{R}_h \geq F(\mathcal{R}_{v0})$ . Observe that as  $\mathcal{R}_{v0}$  increases the critical value of  $\mathcal{R}_h$  diminishes

### 3.1.1 Bistability

For parameters in a certain region, both the disease-free equilibrium  $E_0$  and the interior equilibrium  $\hat{E}_+$  are locally asymptotically stable at the same time. Therefore, initial conditions determine whether the disease will persist or die out. This is clearly a consequence of linking the two processes.

It is easy to verify that the infection-free equilibrium  $E_0$  is always locally asymptotically stable (see supplementary material). The stability of interior equilibria  $\hat{E}_{\pm}$  is more difficult to prove. We have obtained some results by using the time scale argument, which assumes that the within-host dynamics occurs on a faster time scale than the between-host dynamics. The same assumption has also been made in Gilchrist and Coombs [7]. Under this assumption (together with the assumption that  $\hat{E}_{\pm}$  exist), we can first solve for the quasisteady states of the cell-virus sub-system from the  $T$ ,  $T^*$ , and  $V$  equation in (12), which will be functions of  $I$  and  $S$ . These quasisteady states can then be substituted in the  $I$  and  $S$  equation to study the stability of the  $SI$  subsystem. The stability result is described below.

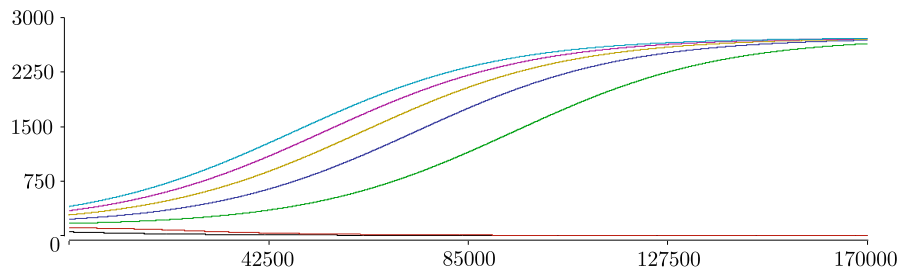
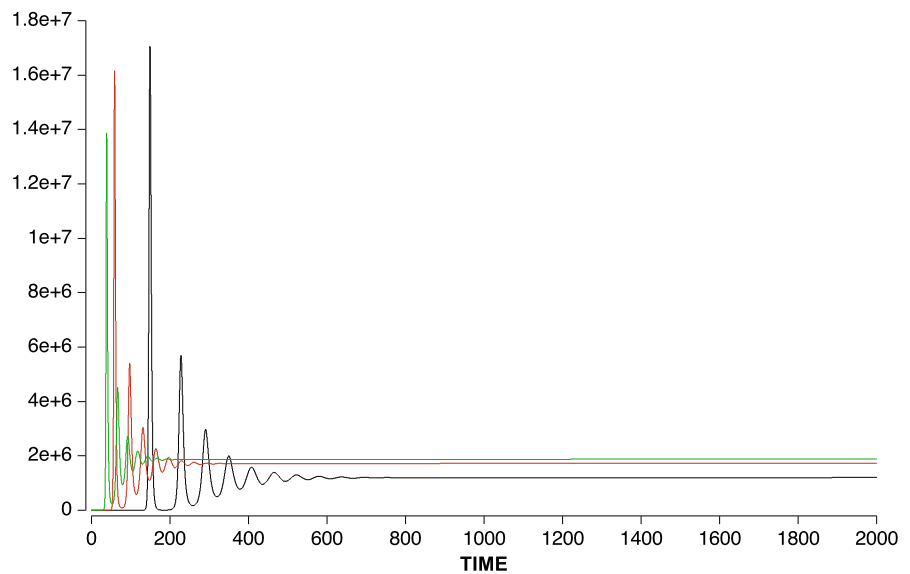


**Fig. 2** Time plot of the solutions (the  $I(t)$  component) of (12). It shows that solutions may converge to either the interior equilibrium  $\hat{E}_+$  or the trivial equilibrium depending on the ini-

tial condition. This suggests that  $\hat{E}_+$  is l.a.s. and  $\hat{E}_-$  is unstable. Parameter values used in simulations are selected such that  $\mathcal{R}_h > F(\mathcal{R}_{v0})$

**Fig. 3** Time plot of the solutions ( $V(t)$  component) of (12), for different values of the initial condition. It shows that whereas  $I$  is increasing, the maximal value for  $V$  is decreasing. Parameter values used in simulations are selected such that  $\mathcal{R}_h > F(\mathcal{R}_{v0})$



**Corollary 2** Let  $\mathcal{R}_{ve}^- > 1$  (or equivalently  $\frac{\hat{I}_-}{N} \mathcal{R}_{v0} > 1$ ) and let the condition (i)(c) in Corollary 1 hold, under which (12) has two interior equilibria  $\hat{E}_\pm$ . Then

- (i)  $\hat{E}_-$  is always unstable;
- (ii)  $\hat{E}_+$  is always locally asymptotically stable

A proof of Corollary 2 can be found in the supplementary material. We remark that although the local stability for  $\hat{E}_\pm$  is obtained by assuming that the within-host dynamics occur on a faster time scale, our numerical simulations of the full system (12), as shown in Fig. 2 suggest that the stability results hold in general. Figure 3 illustrates that solutions can converge to either  $E_0$  or  $\hat{E}_+$ , depending on the initial condition, and that  $\hat{E}_-$  is unstable.

The implications of the bistability are twofold. The first implication is that whether the infections will per-

sist or die out cannot be completely determined by either subsystems alone. More specifically, the disease extinction depends on the threshold condition  $\mathcal{R}_h < F(\mathcal{R}_{v0})$  (see Fig. 1), which involves both between-host property ( $\mathcal{R}_h$ ) and within-host property ( $\mathcal{R}_v$ ). The second implication is that the assumption on the dependence of the within-host force-of-infection on the between-host level of infection ( $kIV$ ) may need to be further explored. Other forms can be considered to examine the robustness of the bistability.

### 4 Discussion

The model presented here has the distinctive property that the infection rates  $\beta$  and  $k$  are linear functions of the viral load  $V$  and prevalence  $I$ , respectively. Although a saturating function might be considered more



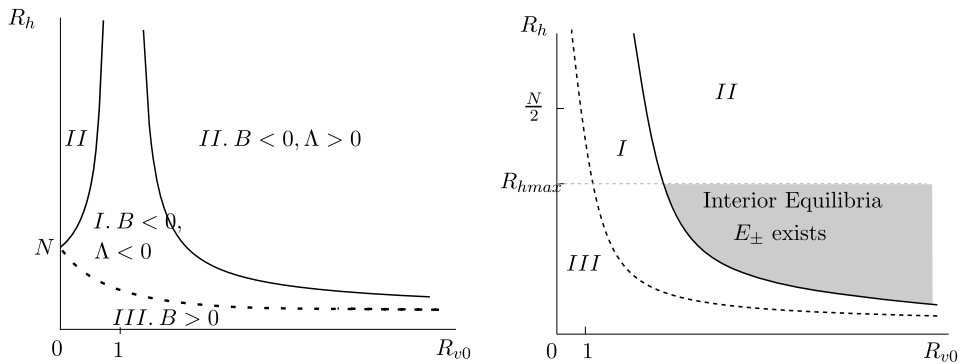


**Fig. 4** Plots of  $F(\mathcal{R}_{v0}) = \hat{N}/(\sqrt{\mathcal{R}_{v0}} - 1)^2$  (the solid curve) and  $G(\mathcal{R}_{v0}) = \hat{N}/(\mathcal{R}_{v0} + 1)$  (the dashed curve), and the three regions in the  $(\mathcal{R}_{v0}, \mathcal{R}_h)$  plane separated by these curves. These regions determine the properties of the solutions  $\hat{y}_{\pm} = \hat{I}_{\pm}/\hat{N}$  of (15).  $\Delta = B^2 - 4\mathcal{R}_{v0}$  is the discriminant of (15) and  $B$  is given in (16). Figure (A) illustrates that  $\mathcal{R}_{v0} = 1$  is an asymptote for

$F(\mathcal{R}_{v0})$  from both sides. It is indicated (by the signs of  $B$  and  $\Delta$ ) that there are no real solutions in Region I; two positive solutions in Region II with  $\mathcal{R}_{ve}^{\pm} > 1$  ( $\hat{V}_{\pm} \leq 0$  for  $\mathcal{R}_{ve}^{\pm} \leq 1$ ); and no positive solutions in Region III. Figure (B) is an enlarged version of (A) for the subregion of II in which interior equilibria  $\hat{E}_{\pm}$  exist

realistic, we note that the dependence on  $I$  or  $V$  is more important at low level of infection when the coupling of within- and between-host dynamics is most relevant. When the system is near the endemic equilibrium,  $\beta$  and  $k$  are largely independent of  $V$  and  $I$ ; and thus, the coupling of the two systems becomes weaker.

Our model provides two threshold quantities,  $\mathcal{R}_v$  (or  $\mathcal{R}_{v0}$ ) and  $\mathcal{R}_h$ , which correspond to the within-host and between-host dynamics, respectively. The magnitudes of these quantities can jointly determine the prevalence of an infection. This is a direct consequence of the coupling of the two processes. The dependence of disease outcomes on  $\mathcal{R}_v$  and  $\mathcal{R}_h$  is illustrated in Fig. 4.

It shows in Fig. 5 that a stable interior equilibrium exists for  $(\mathcal{R}_v, \mathcal{R}_h)$  in the region above the solid curve (Region II), while only the DFE exists for  $(\mathcal{R}_v, \mathcal{R}_h)$  in the region below the dashed curve (Region III). Note that a virus with large  $\mathcal{R}_{v0}$  can spread in a population even for relatively low values of  $\mathcal{R}_h$ . On the other hand, when  $\mathcal{R}_{v0}$  is small, the virus may not be successful at the population level. This is because it requires a very large value of  $\mathcal{R}_h$ , e.g., larger than the maximum feasible value  $\mathcal{R}_{hmax}$ . We remark that these results are the consequence of postulating the law of mass action for the average densities of the variables.

We point out that, under usual assumptions, our model reduces to either the well-known *SI* epidemiological model for host population dynamics or the standard viral dynamics model at the individual host level. Both sub-models have been studied extensively

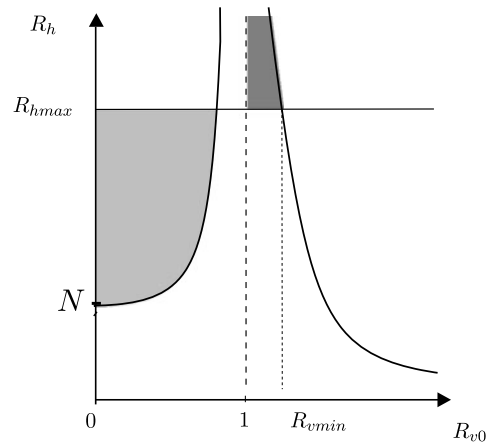


**Fig. 5** Plot of  $\mathcal{R}_h$  as a function of  $\mathcal{R}_{v0}$ . The disease can persist only if parameters are such that the point  $(\mathcal{R}_{v0}, \mathcal{R}_h)$  is above the curve  $\mathcal{R}_h = F(\mathcal{R}_{v0})$  and below  $\mathcal{R}_{hmax}$  (the lightly shaded region). The graph illustrates that when the virus has a high within-host reproduction ( $\mathcal{R}_{v0}$  is large), the disease can persist even when the between-host reproduction number is small. However, when  $\mathcal{R}_{v0}$  is small, a very high  $\mathcal{R}_h$  will be required for the disease to persist. Moreover, when  $\mathcal{R}_{v0}$  is between  $(1, \mathcal{R}_{vmin})$ , it is impossible for the disease to persist even if  $\mathcal{R}_h$  is high. This is a “dangerous zone” for the virus (the darker region)

and shown to have standard dynamics. That is, each of the two submodels has a usual basic reproductive number that determines whether the infection-free equilibrium is stable or there is a unique stable endemic equilibrium. However, when the two submodels are linked explicitly in both directions, new dynamics may emerge and threshold conditions can be very different.

In particular, the establishment of infection may depend on the initial conditions and, therefore, the sharp threshold condition of classical epidemiological models imposed by  $R_0$  no longer holds.

**Acknowledgements** We thank Suzanne Lenhart for very helpful discussions. MCA thanks Nikola Petrov for the helpful comments. We acknowledge funding from the National Institute for Mathematical and Biological Synthesis through the National Science Foundation EF-0832-858. ZF’s research is partially supported by NSF (DMS-1022758) and by the James S. McDonnell Foundation.

**Appendix: Stability of the coupled model**

In this section we prove the stability of  $E_{\pm}$  for the coupled model.

The Jacobian matrix at  $E_{\pm} = (\hat{S}_{\pm}, \hat{I}_{\pm}, \hat{T}_{\pm}, \hat{T}^*_{\pm}, \hat{V}_{\pm})$ , is

$$J_{\pm} = \begin{bmatrix} -a_{1\pm} - \mu & -\mu & 0 & 0 & -a_{2\pm} \\ a_{1\pm} & 0 & 0 & 0 & a_{2\pm} \\ 0 & -a_{3\pm} & -a_{4\pm} - \mu c & 0 & -a_{5\pm} \\ 0 & a_{3\pm} & a_{4\pm} & -(\mu c + \delta_c) & a_{5\pm} \\ 0 & 0 & 0 & p & -c \end{bmatrix}.$$

where

$$\begin{aligned} a_{1\pm} &= \frac{\mu \mathcal{R}_h}{N} (\mathcal{R}_{v0} \hat{y}_{\pm} - 1), \\ a_{2\pm} &= \beta N^2 y_{\pm} (1 - y_{\pm}), \\ a_{3\pm} &= k \hat{T}_{\pm} \hat{V}_{\pm}, \\ a_{4\pm} &= \mu c (\mathcal{R}_{v0} \hat{y}_{\pm} - 1), \\ a_{5\pm} &= \frac{T_0 k N}{\mathcal{R}_{v0}}. \end{aligned} \tag{23}$$

Then, the characteristic polynomial associated to  $J_{\pm}$  is

$$(X + \mu)(X^4 + A_3 X^3 + A_2 X^2 + A_1 X + A_0)$$

where

$$\begin{aligned} A_3 &= a_{1\pm} + c + \delta_c + \mu c (1 + \mathcal{R}_{v0} \hat{y}_{\pm}) > 0 \\ A_2 &= (a_{1\pm} + \mu c \mathcal{R}_{v0} \hat{y}_{\pm})(c + \delta_c + \mu c) \\ &\quad + a_{1\pm} \mu c \mathcal{R}_{v0} \hat{y}_{\pm} > 0 \\ A_1 &= \left[ \frac{\mathcal{R}_h \mu \mu c}{N} (c + \delta_c + \mu c) \mathcal{R}_{v0} \hat{y}_{\pm} \right. \\ &\quad \left. + \frac{T_0 k p N \mu c}{\mathcal{R}_{v0}} \right] [\mathcal{R}_{v0} \hat{y}_{\pm} - 1] - \frac{T_0 k p N \mu}{\mathcal{R}_{v0}} \\ A_0 &= \frac{T_0 k p N \mu \mu c}{\mathcal{R}_{v0} (1 - y_{\pm})} \hat{y}_{\pm} (2 \mathcal{R}_{v0} \hat{y}_{\pm} + B) \end{aligned} \tag{24}$$

where  $B$  is given in (16). Considering (19) we get  $A_0 < 0$  for  $E_-$  and  $A_0 > 0$  for  $E_+$ . Hence,  $E_-$  is always unstable, the stability for  $E_+$  is determined by sign of  $A_1$ .

A necessary condition for the stability of  $E_+$  is given by  $A_1 \geq 0$ , otherwise we have roots with positive real part. Now, for  $E_+$ ,  $A_1 = 0$  we obtain a quadratic equation for  $\mathcal{R}_{ve}^+ = \mathcal{R}_{v0} \hat{y}_+$  which has a positive real root (larger than 1) that we label  $R_{E_+}$  and a negative real root. Then, we have the result

**Lemma** *When  $E_{\pm}$  exist,  $E_-$  is always unstable, while  $E_+$  is l.a.s. if  $\mathcal{R}_{ve}^+ \geq R_{E_+} > 1$  and  $A_1 A_2 A_3 > A_1^2 + A_3^2 A_0$ , otherwise  $E_+$  is unstable.*

**References**

1. Anderson, R.M., May, R.M.: Infectious Diseases of Humans. Oxford University Press, Oxford (1991)
2. Callaway, D., Perelson, A.: HIV-1 infection and low steady state viral loads. *Bull. Math. Biol.* **64**, 29–64 (2002)
3. Coombs, D., Gilchrist, M.A., Ball, C.L.: Evaluating the importance of within- and between-host selection pressures on the evolution of chronic pathogens. *Theor. Popul. Biol.* **72**, 576–591 (2007)
4. De Boer, R.J., Perelson, A.S.: Target cell limited and immune control models of HIV infection: a comparison. *J. Theor. Biol.* **190**, 201–214 (1998)
5. Dixit, N., Perelson, A.: Complex patterns of viral load decay under antiretroviral therapy: influence of pharmacokinetics and intracellular delay. *J. Theor. Biol.* **226**, 95–109 (2004)
6. Fraser, C., Hollingsworth, T.D., Chapman, R., de Wolf, F., Hanage, W.P.: Variation in HIV set-point viral load: Epidemiological analysis and an evolutionary hypothesis. *Proc. Natl. Acad. Sci. USA* **104**(44), 17441–17446 (2007)
7. Gilchrist, M.A., Coombs, D.: Evolution of virulence: interdependence, constraints, and selection using nested models. *Theor. Popul. Biol.* **69**, 145–153 (2006)
8. Markowitz, M., Vesanen, M., Tenner-Racz, K., Cao, Y., Binley, J.M., Talai, A., et al.: A novel antiviral intervention results in more accurate assessment of human immunodeficiency virus type 1 replication dynamics and T-cell decay in vivo. *J. Virol.* **77**, 5037–5038 (2003)
9. Nowak, M.A., May, R.M.: Mathematical biology of HIV infectious-antigenic variation and diversity threshold. *Math. Biosci.*, **106**, 1–21 (1991)
10. Nowak, M.A., May, R.M.: Virus Dynamics. Mathematical Principles of Immunology and Virology. Oxford University Press, Oxford (2000)
11. Perelson, A., Kirschner, D., De Boer, R.: The dynamics of HIV infection of CD4+ T cells. *Math. Biosci.* **114**, 81–125 (1993)
12. Perelson, A., Nelson, P.W.: Mathematical analysis of HIV-1 dynamics in vivo. *SIAM Rev.* **41**, 3–44 (1999)

13. Ramratnam, B., Bonhoeffer, S., Binley, J., Hurley, A., Zhang, L., Mittler, J.E., et al.: Rapid production and clearance of HIV-1 and hepatitis C virus assessed by large volume plasma apheresis. *Lancet* **354**, 1782–1785 (1999)
14. Regoes, R.R., Wodarz, D., Nowak, M.A.: Virus Dynamics: the effect of target cell limitation and immune response on virus evolution. *J. Theor. Biol.* **191**, 451–462 (1998)
15. Thieme, H.R.: *Mathematics in Population Biology*. Princeton Series in Theoretical and Computational Biology. Princeton University Press, Princeton (2003)
16. Wodarz, D.: *Killer Cell Dynamics. Mathematical and Computational Approach to Immunology*. Interdisciplinary Applied Mathematics, vol. 32. Springer, Berlin (2007)